



**Full Length Article**

## Implications of nrDNA and cpDNA Region in *Acer* (Aceraceae): DNA Barcoding and Phylogeny

Li Lin<sup>1,2</sup>, Zhiyong Zhu<sup>2</sup>, Lejing Lin<sup>2</sup>, Benke Kuai<sup>1</sup>, Yulong Ding<sup>1,3\*</sup> and Tiantian Du<sup>2</sup>

<sup>1</sup>Co-Innovation Center for Sustainable Forestry in Southern China, College of Biology and the Environment, Nanjing Forestry University, Nanjing 210037, PR China

<sup>2</sup>Ningbo City College of Vocational Technology, Ningbo 315502, PR China

<sup>3</sup>Co-Innovation Center for Sustainable Forestry in Southern China, Bamboo Research Institute, Nanjing 210037, PR China

\*For correspondence: linli851111@163.com

### Abstract

*Acer* Linn. (Aceraceae), is a genus of the most important horticultural trees. Many species in this genus are potential medicinal plants. However, *Acer* species are easily confused for their similar morphological features, and therefore the phylogenetic relationships among *Acer* species are not fully understood. This hinders the new varietal breeding and genetic resource preservation. Here, six candidate DNA barcodes (*psbA-trnH*, *matK*, *trnL-trnF*, *rbcL*, ITS2 and ITS) were evaluated for the ability to identify 69 species in *Acer*. For evaluating each barcode's ability to identify species, PCR amplification and sequencing efficiency, genetic divergence, DNA barcoding gaps and discrimination success rates were assessed. The results indicated that ITS region was suitable barcode, ITS sequence exhibited significant inter- and intra-specific variation, clear DNA barcoding gaps, and higher species identification efficiency (73.09% for “all species barcodes” analysis). In addition, Phylogenetic tree was constructed based on 171 ITS sequences from 51 *Acer* species. Species clusters observed in the trees largely agreed with morphologically-based taxa of Xu *et al.* (2013) 14 sections, and 12 sections were supported in the ML tree. However, the taxonomic status of several species should be further analyzed, such as *A. yangbiense*, *A. crassum*, *A. wardii*. Our results showed that ITS region can be used as an efficient and efficient tool for identifying the species and phylogenetic analysis of *Acer*. © 2019 Friends Science Publishers

**Key words:** *Acer*; DNA barcoding; ITS; Molecular identification; Phylogenetic relationship

### Introduction

*Acer* Linn., a wide spread genus in the family Aceraceae, contains approximately 129 species distributing in temperate and tropical mountain ranges of the Northern Hemisphere (Xu *et al.*, 2013). Of which more than three quarters have been found in China, including 99 species (61 endemic), classified into 14 sections (Xu *et al.*, 2013). Many *Acer* species have important horticultural and economical values and some species, including *A. tataricum* subsp. *ginnala*, *A. tegmentosum* and *A. saccharum* are widely planted for their beautiful autumn colors, medicinal components, or raw sugar product (Tung *et al.*, 2008; Yuan *et al.*, 2011). *Acer* species have very significant morphological features that are their samaras with an elongated wing, while some other characters, such as leaf shapes and inflorescence types, are very diverse (Sipe and Linnerooth, 1995; Xu, 1996a, b; Tian *et al.*, 2002). Although the leaf shapes of most *Acer* species are simple and palmately lobed, the number of lobes is variable, even in intraspecies, such as *A. amplum*, with 3- or 5-lobed or unlobed (Tanai, 1978; Tian *et al.*, 2002; Xu *et al.*, 2013). Several types of inflorescence, such as corymbiform,

umbelliform, racemose and large paniculate, occur in this genus (Tian *et al.*, 2002; Xu *et al.*, 2013). Variation in samaras shapes and blended sexuality types are also represented in this genus (Sipe and Linnerooth, 1995; Xu, 1996a; Xu *et al.*, 2013). These variances make the taxonomy of *Acer* species very difficult by analyzing gross morphology (Xu, 1998; Xu *et al.*, 2013; Gao *et al.*, 2015). In addition, the species delimitation and phylogenetic relationships in this genus are also very controversial, although some evidence, including morphological characters, chemical composition, geographical distributions, fossils and molecular data, are available (Tian *et al.*, 2002).

Molecular data has been induced in taxonomy, systematics and evolutionary biology for more than 20 years, which provided an unprecedented way to explore the width and depth of biodiversity (Fay *et al.*, 1998; Hebert *et al.*, 2003a,b; Ren *et al.*, 2009). However, there are still millions of species that await description, and plant identification remains a great challenge (Mora *et al.*, 2016). DNA barcoding, based on DNA sequencing from a standardized genome region, has proved an effective approach for species identification, biodiversity assessment,

phylogenetic analysis, new and cryptic species investigation, and natural resources conservation (Hebert and Gregory, 2005; Lee *et al.*, 2016; Feng *et al.*, 2016). DNA barcode provides lots of advantages: (1) no request on morphological information; (2) not affected by environmental factors and individual growth habitats; (3) fast and easy to operate; and (4) available for identification of large number of samples (Wyler and Naciri, 2016). For animals, the mitochondrial *cytochrome c oxidase I (COI)* gene has been recognized as the official DNA barcode (Hebert and Gregory, 2005), although some other mitochondrial loci were also been proved effective for some taxa (*e.g.*, Vences *et al.*, 2005). For plants, several nrDNA and cpDNA regions, including *matK*, *atpF-atpH*, *rbcL*, *rpoB*, *ycf1*, *psbA-trnH*, *trnL-trnF*, ITS and ITS2, were proposed for potential standard DNA barcoding, but no consensus has been reached until now (Kress *et al.*, 2005; Luo *et al.*, 2010; Chen *et al.*, 2010; Feng *et al.*, 2016). In 2009, the CBOL Plant Working Group suggested *rbcL* and *matK* as the core barcodes for plants, while Ren *et al.* (2009) and Yu *et al.* (2011a) demonstrated that the internal transcribed spacer (ITS) was a better choice for some plants taxa. For short length and high PCR efficiency, ITS2 was considered as a more suitable barcode marker than ITS (Yao *et al.*, 2010; Feng *et al.*, 2016). Some authors found that *trnL-trnF* and *psbA-trnH* were also two promising DNA barcoding loci (*e.g.*, Wyler and Naciri, 2016; Wang, *et al.*, 2016). These differences indicated that further testing of DNA barcodes across more species and more plant taxa should be carried out.

At present, some DNA marker systems, including RAPD, AFLP, SRAP, SSR and ISSR, have been served to genetically analyze *Acer* species (Li, *et al.*, 2010; Chen *et al.*, 2011; Lin, *et al.*, 2015). In addition, two DNA sequences, ITS and *trnL-trnF* regions, have been applied to reconstruct the phylogeny of Aceraceae (Tian *et al.*, 2002; Grimm *et al.*, 2006). Although the combination of *rpl16 + psbA-trnH+trnL-trnF* was considered to be useful for taxa identification at the intraspecific level in *A. palmatum* (Gao *et al.*, 2015), no one has extensively evaluated the *Acer* genus at interspecific level. Here, we tested six candidate DNA barcoding fragments (*rbcL*, *matK*, *trnH-psbA*, *trnL-trnF*, ITS2, and ITS) to explore a most suitable DNA barcode for different species in the genus *Acer*, and then used it to construct the phylogenetic relationships among *Acer* species.

## Materials and Methods

### Sample Collection

In order to select the most suitable barcoding fragment for *Acer* species, we collected totally 427 samples belonging to 69 species in this study. Fifty two specimens of 41 species were sampled in eight provinces and three municipality of China including Guangxi, Yunnan, Zhejiang, Hubei, Liaoning, Jiangxi, Jiangsu, Henan, Chongqing, Beijing,

and Shanghai (Table 1). All samples were identified to species using the herbarium specimen and botanical information from Chinese Virtual Herbarium (<http://www.cvh.org.cn/>). Digital image information and voucher specimens of these species were stored in the herbarium of Ningbo City College of Vocational Technology. Additionally, 375 sequences were downloaded from GenBank, which comprised 61 *Acer* species (Table S1). Because the delimitation of some *Acer* species was controversial, we followed the latest classification criteria of Flora of China (Xu *et al.*, 2013) in this study.

### DNA Extraction, Amplification and Sequencing

Total DNA was extracted from dried leaf tissue using the plant/Fungal DNA Miniprep Kit (Lifefeng Biotech Co., Shanghai, China). The PCR reactions were performed on an AG 22331 Hamburg Mastercycler (Eppendorf Ltd., Hamburg, Germany). Primers used for amplification and DNA sequencing were given in Table 2. The amplification reactions were carried out in 50  $\mu$ L volumes containing 100 ng template DNA, 1  $\mu$ L of each primer (10  $\mu$ mol/L), 25  $\mu$ L 2  $\times$  Taq PCR MasterMix (BioTeke Corporation, Beijing, China), and 22  $\mu$ L ddH<sub>2</sub>O. The cycling conditions were obtained from White *et al.* (1990) and Chen *et al.* (2010). All PCR products were purified using AxyPrep PCR Cleanup Kit (Axygen Biotechnology Limited, Hangzhou, China), and then sequenced using an ABI 3730xl DNA Analyzer (Applied Biosystems, CA, USA). Newly generated sequences were lodged in GenBank, and accession numbers were allocated (Table 1).

### Data Analyses

The raw sequences were assembled manually using Vector NTI software (Invitrogen Inc., Carlsbad, CA, USA). Sequences containing ITS2 were trimmed and retrieved according to Chen *et al.* (2010). All *psbA-trnH* and *trnL-trnF* regions were edited and generated according to GenBank annotations. All sequences alignment and checking were produced using Clustal X 2.1. Kimura 2-Parameter (K2P) distances were calculated in MEGA version 6.0 (Tamura *et al.*, 2013). Three parameters were applied to characterize the inter-specific divergence (Meyer and Paulay, 2005; Feng *et al.*, 2016): average inter-specific distance, theta prime, and minimum inter-specific distance. Another three different parameters were used to evaluate the intra-specific variability (Chen *et al.*, 2010; Gao *et al.*, 2010a): average intra-specific distance, theta and coalescent depth. DNA barcoding gaps were evaluated by comparing the distribution of intra-versus inter-specific distances (Slabbinck *et al.*, 2008; Feng *et al.*, 2016) and Wilcoxon signed-rank tests were used as described previously (Feng *et al.*, 2016). In order to further evaluated the effectiveness of each potential DNA barcode, three criteria (Best Match: BM; Best Close Match: BCM; and All Species Barcodes:

**Table 1:** Samples information of *Acer* species

| genera             | Section  | Samples name                                 | Sampling location                       | Voucher number                   | GenBank Accession no. |             |             |                  |                  |          |
|--------------------|--|--|---|----------------------------------|-----------------------|-------------|-------------|------------------|------------------|----------|
|                    |  |  |   |                                  | ITS                   | <i>matK</i> | <i>rbcl</i> | <i>trnH-psbA</i> | <i>trnL-trnF</i> |          |
| <i>Acer</i>        | Platanoidea                                      | <i>A. miaotaiense</i>                        | Chenshan, Shanghai                      | AM2015SH02                       | KU902468              | KU902505    | KU902585    | KU945298         | KU749519         |          |
|                    |  | <i>A. miaotaiense</i>                        | Taoyuanling, Hangzhou, Zhejiang         | AY2015HZ05                       | KU902489              | KU902509    | KU902597    | KU945299         | KU749540         |          |
|                    |  | <i>A. miaotaiense</i>                        | Shennongjia Forestry District, Hubei    | AY2015WH07                       | KU902490              | KU902508    | KU902598    | KU945300         | KX494388         |          |
|                    |  | <i>A. truncatum</i>                          | Yaowan, Wuhan, Hubei                    | KU902494                         | KU902538              | KU902600    | KU945301    | KU749493         |                  |          |
|                    |  | <i>A. Pictum</i> subsp. <i>mono</i>          | Mt. Tianmu, Hangzhou, Zhejiang          | AM2015HZ10                       | KX494362              | KU902542    | KU902589    | KU945342         | KU749528         |          |
|                    |  | <i>A. acutum</i>                             | Fragrance Hill, Beijing                 | AA2015BJ01                       | KU902474              | KU902515    | KU902587    | KU945303         | KX494394         |          |
|                    |  | <i>A. acutum</i>                             | Chenshan, Shanghai                      | AA2015SH03                       | KU902473              | KU902514    | KU902586    | KU945304         | KX494393         |          |
|                    |  | <i>A. acutum</i>                             | Mt. Tianmu, Hangzhou, Zhejiang          | AA2015HZ02                       | KU902475              | KU902516    | KU902588    | KU945302         | KU749526         |          |
|                    |  | <i>A. cappadocicum</i> subsp. <i>sinicum</i> | Kunming, Yunnan                         | AC2015KM06                       | KU902486              | KU902534    | KU902591    | KU945305         | KU749536         |          |
|                    |  | <i>A. amplum</i> subsp. <i>tientaiense</i>   | Mt. Tiantai, Taizhou, Zhejiang          | AA2015HZ08                       |                       | KU902531    | KU902618    | KU945339         | KU749531         |          |
|                    |  | Palmata                                      | <i>A. palmatum</i>                      | Xikou, Fenghua, Zhejiang         | AP2015FH07            | KU902463    | KX494366    | KX494375         | KU945341         | KU749507 |
|                    |  |  | <i>A. japonicum</i>                     | Chenshan, Shanghai               | AJ2015SH10            | KX494352    | KU902537    | KX494376         | KU945343         | KU749542 |
|                    |  |  | <i>A. pseudosieboldianum</i>            | Kuandian, Dandong, Liaoning      | AP2015LN04            | KX494353    | KU902561    | KU902576         | KU945340         | KU749508 |
|                    |  |  | <i>A. sinense</i>                       | Hangzhou, Zhejiang               | AS2015HZ06            | KU902493    | KU902544    | KU902599         | KU945312         | KU749547 |
|                    |  |  | <i>A. flabellatum</i>                   | Hangzhou, Zhejiang               | AF2015HZ05            | KU902482    | KU902529    | KU902590         | KU945311         | KU749529 |
|                    | <i>A. elegantulum</i>                            |  | Yanshan, Guilin, Guangxi                | AO2015GL01                       | KU902460              | KU902522    | KU902570    | KU945345         | KX494389         |          |
|                    | <i>A. elegantulum</i>                            |  | Kunming, Yunnan                         | AO2015KM01                       | KU902461              | KU902523    | KU902571    | KU945346         | KU749499         |          |
|                    | <i>A. elegantulum</i>                            |  | Mt. Tianmu, Hangzhou, Zhejiang          | AE2015HZ04                       | KU902487              | KU902562    | KU902596    | KX494382         | KU749538         |          |
|                    | <i>A. elegantulum</i>                            |  | Mt. Siming, Ningbo, Zhejiang            | AE2015NB01                       | KU902488              | KU902563    | KX870504    | KU945316         | KU749546         |          |
|                    | <i>A. pubinerve</i>                              |  | Chenshan, Shanghai                      | AP2015SH12                       | KX494354              | KU902558    | KU902584    | KU945313         | KU749518         |          |
|                    | <i>A. oliverianum</i>                            |  | Wuhan, Hubei                            | AO2015WH06                       | KU902485              | KU902532    | KU902593    | KU945315         | KU749533         |          |
|                    | <i>A. wilsonii</i>                               |  | Chenshan, Shanghai                      | AW2015SH04                       | KU902481              | KX494367    | KX494377    | KU945347         | KU749527         |          |
|                    | <i>A. fenzelianum</i>                            |  | Moshan, Wuhan, Hubei                    | AF2015WH09                       |                       | KU902521    | KU902602    | KU945358         | KU749505         |          |
|                    | <i>A. fabri</i>                                  |  | Yanshan, Guilin, Guangxi                | AF2015GL03                       | KU902465              | KU902524    | KU902575    | KX494383         | KU749506         |          |
|                    | <i>A. fabri</i>                                  |  | Wuhan, Hubei                            | AF2015WH04                       | KU902466              | KU902525    | KU902574    | KU945324         | KU749517         |          |
|                    | Oblonga  | <i>A. pauciflorum</i>                        | Mt. Zhongshan, Nanjing, Jiangsu         | AC2015NJ03                       | K494349               | KU902549    | KU944372    | KU945308         | KU749496         |          |
|                    |  | <i>A. buergerianum</i>                       | Kunming, Yunnan                         | AB2015KM04                       | KU902480              | KU902512    | KU902580    | KU945320         | KU749513         |          |
|                    |  | <i>A. buergerianum</i>                       | Fragrance Hill, Beijing                 | AB2015BJ02                       | KU902477              | KU902510    | KU902578    | KU945317         | KX494390         |          |
|                    |  | <i>A. buergerianum</i>                       | Mt. Lushan, Jiujiang, Jiangxi           | AB2015LS02                       | KU902479              | KU902513    | KU902581    | KU945318         | KX494392         |          |
|                    |  | <i>A. buergerianum</i>                       | Xikou, Fenghua, Zhejiang                | AB2015FH02                       | KU902478              | KU902511    | KU902579    | KU945319         | KX494391         |          |
|                    |  | <i>A. paxii</i>                              | Kunming, Yunnan                         | AP2015KM02                       | KU902464              | KU902504    | KU902577    | KU945321         | KU749511         |          |
|                    |  | <i>A. coriaceifolium</i>                     | Kunming, Yunnan                         | AC2015KM08                       | KU902492              | KU902543    | KU902601    | KU945322         | KU749545         |          |
|                    |  | <i>A. oblongum</i>                           | Yaowan, Wuhan, Hubei                    | AO2015WH02                       | KU902459              | KU902546    | KU902565    | KU945348         | KU749486         |          |
|                    |  | Macrantha                                    | <i>A. davidii</i> subsp. <i>grosser</i> | Anning District, Kunming, Yunnan | AG2015KM10            | KX494355    | KU902519    | KU902609         | KU945327         | KU749500 |
|                    |  |  | <i>A. davidii</i>                       | Kunming, Yunnan                  | AD2015KM03            | KU902471    | KX494368    | KU902613         | KU945351         | KU749524 |
|                    |  |  | <i>A. sikkimense</i>                    | Taoyuanling, Hangzhou, Zhejiang  | AH2015HZ01            | KU902472    | KU902541    | KU902614         | KU945326         | KU749525 |
|                    |  |  | <i>A. metcalffii</i>                    | Nanshan, Chongqing               | AM2015CQ02            |             | KU902506    | KU902608         | KX494384         | KU749520 |
|                    |  |  | <i>A. pectinatum</i>                    | Kunming Botanical Garden, Yunnan | AP2015KM15            | KX494356    | KX494369    | KX494378         | KX494385         | KU749491 |
|                    |  | Lithocarpa                                   | <i>A. tegmentosum</i>                   | Kuandian, Dandong, Liaoning      | AT2015LN01            | KU902470    | KU902540    | KU902616         | KU945328         | KU749523 |
|                    |  |  | <i>A. sinopurpurascens</i>              | Taoyuanling, Hangzhou, Zhejiang  | AS2015HZ03            | KU902483    | KU902530    | KU902603         | KU945329         | KU749487 |
|                    | <i>A. tsinglingense</i>                          |  | MT. Funiu, Luanchuan, Henan             | AT2015HN05                       | KU902469              | KU902539    | KX494379    | KU945352         | KU749488         |          |
|                    | <i>A. sterculiaceum</i> subsp. <i>franchetii</i> |  | Fangxian, Shiyuan, Hubei                | AF2015WH01                       | KU902458              | KU902518    | KU902606    | KU945330         | KU749498         |          |
|                    | <i>A. kangshanense</i>                           |  | Kunming Botanical Garden, Yunnan        | AK2015KM11                       | KX494357              | KU902520    | KX494380    | KU945354         | KU749501         |          |
|                    | Ginnala  | <i>A. yangbiense</i>                         | Kunming Botanical Garden, Yunnan        | AY2015KM07                       | KU902491              |             | KU902623    | KU945335         | KU749541         |          |
|                    |  | <i>A. tataricum</i> subsp. <i>ginnala</i>    | Xuhui, Shanghai                         | AG2015SH06                       | KU902495              | KU902555    | KU902582    | KU945309         | KU749495         |          |
| Pentaphylla        |  | <i>A. pentaphyllum</i>                       | Kunming Botanical Garden, Yunnan        | AP2015KM12                       | KX494358              | KU902533    | KU902619    | KU945331         | KU749534         |          |
|                    |  | Trifoliata                                   | <i>A. griseum</i>                       | Mt. Zhongshan, Nanjing, Jiangsu  | AG2015NJ02            | KX494359    | KU902527    | KU902622         | KU945332         | KU749539 |
| <i>A. nikoense</i> |  |  | Mt. Lushan, Jiujiang, Jiangxi           | AN2015LS01                       | KU902467              | KU902526    | KU902620    | KU945355         | KX494387         |          |
| Negundo            | <i>A. triflorum</i>                              | Kuandian, Dandong, Liaoning                  | AT2015LN02                              | KU902476                         | KU902507              | KU902615    | KU945333    | KU749521         |                  |          |
|                    | <i>A. mandshuricum</i>                           | Kuandian, Dandong, Liaoning                  | AM2015LN03                              | KX494360                         | KU902528              | KU902605    | KU945356    | KU749490         |                  |          |
|                    | <i>A. henryi</i>                                 | MT. Funiu, Luanchuan, Henan                  | AH2015SH08                              | KX494361                         | KU902503              | KU902611    | KU945334    | KU749510         |                  |          |
|                    | <i>A. negundo</i>                                | Xuhui, Shanghai                              | AN2015SH01                              | KU902456                         | KX494370              | KU902606    | KU945357    | KU749493         |                  |          |
|                    | Dipteronia                                       | <i>D. sinensis</i>                           |   | GenBank                          | AY605290              |             |             |                  |                  |          |
| <i>D. sinensis</i> |  |  | GenBank                                 | EU720445                         |                       |             |             |                  |                  |          |
| <i>D. sinensis</i> |  |  | GenBank                                 | AF401121                         |                       |             |             |                  |                  |          |

ASB) were calculated for each alignment using the software Taxon DNA (Slabbinck *et al.*, 2008; Lee *et al.*, 2016). Phylogenetic trees were generated using MEGA version 6.0 based on the maximum likelihood (ML) method (Tamura *et al.*, 2013). Bootstrap values were computed using 1000 replicates. Three *Dipteronia sinensis* samples were used as outgroups (Table 1).

## Results

### Character Analysis of Each Barcode

We obtained 49 ITS/ITS2, 51 *matK*, 52 *rbcl*, 52 *trnH*–

*psbA*, and 52 *trnL*–*trnF* sequences from the 52 *Acer* samples. The amplification success rate of all five regions was 100%. The percentage of successful sequencing was 100% for *rbcl*, *trnH*–*psbA* and *trnL*–*trnF*, 98.08% for *matK*, and 94.23% for ITS/ITS2 (Table 3). The aligned lengths of the six DNA sequences ranged from 277 bp (ITS2) to 705 bp (ITS) (Table 3). Among the six DNA barcodes, ITS2 exhibited the highest percentage (49.46%) of variable sites (Table 3). Among the plastid barcodes, the non-coding region *trnH*–*psbA* had the highest percentage of variable sites, which was approximately 3.1, 1.4 and 5.4 times more variable than *matK*, *trnL*–*trnF* and

**Table 2:** Primers used for PCR in this study

| DNA region      | Primer | Sequence                          | Reference              |
|-----------------|--------|-----------------------------------|------------------------|
| ITS             | ITS4   | 5'-TCCTCCGCTTATTGATATG-3'         | White et al., 1990     |
|                 | ITS5   | 5'-GGAAGTAAAAGTCGTAACAAGG-3'      | White et al., 1990     |
| <i>matK</i>     | 472F   | 5'-CCCRTYCATCTGGAAATCTTGGTTC-3'   | Yu et al., 2011b       |
|                 | 1248R  | 5'-GCTRTRATAATGAGA AAGATTCTGTC-3' | Yu et al., 2011b       |
| <i>rbcL</i>     | 1F     | 5'-ATGTCACCACAAACAGAAAC-3'        | Olmstead et al., 1992  |
|                 | 724R   | 5'-TCGCATGTACCTGCAGTAGC-3'        | Fay et al., 1998       |
| <i>tmH-psbA</i> | tmH    | 5'-CGCGCATGGTGGATTCACAATCC-3'     | Tate and Simpson, 2003 |
|                 | psbA   | 5'-GTTATGCATGAACGTAATGCTC-3'      | Sang et al., 1997      |
| <i>tmL-trnF</i> | tmL    | 5'-CGAAATCGGTAGACGCTACG-3'        | Taberlet et al., 1991  |
|                 | trnF   | 5'-ATTGAAGCTGGTGACACGAG-3'        | Taberlet et al., 1991  |

**Table 3:** DNA barcoding utility of six candidate sequences for *Acer*

| Potential barcode | Aligned length (bp) | No. samples species (individuals) | Conserved sites (%) | Variable sites (%) | Informative sites (%) | PCR efficiency (%) | Sequencing efficiency (%) |
|-------------------|---------------------|-----------------------------------|---------------------|--------------------|-----------------------|--------------------|---------------------------|
| ITS               | 705                 | 51(171)                           | 428(60.71)          | 271(38.44)         | 237(33.62)            | 52/52 (100)        | 49/52 (94.23)             |
| ITS2              | 277                 | 51(171)                           | 136(49.10)          | 137(49.46)         | 121(43.68)            | 52/52 (100)        | 49/52 (94.23)             |
| <i>matK</i>       | 691                 | 46(91)                            | 647(93.63)          | 44(6.37)           | 31(4.49)              | 52/52 (100)        | 51/52 (98.08)             |
| <i>rbcL</i>       | 599                 | 51(102)                           | 577(96.33)          | 22(3.67)           | 13(2.17)              | 52/52 (100)        | 52/52 (100)               |
| <i>tmH-psbA</i>   | 511                 | 56(110)                           | 389(76.13)          | 101(19.76)         | 77(15.07)             | 52/52 (100)        | 52/52 (100)               |
| <i>tmL-trnF</i>   | 403                 | 60(158)                           | 332(82.38)          | 55(13.65)          | 42(10.42)             | 52/52 (100)        | 52/52 (100)               |

**Table 4:** Analysis of inter-specific divergence and intra-specific variation of the six candidate barcodes for the whole samples

| Marker                          | ITS           | ITS2          | <i>matK</i>   | <i>rbcL</i>   | <i>psbA-trnH</i> | <i>tmL-trnF</i> |
|---------------------------------|---------------|---------------|---------------|---------------|------------------|-----------------|
| Theta                           | 0.0016±0.0018 | 0.0019±0.0030 | 0.0015±0.0020 | 0.0005±0.0007 | 0.0031±0.0055    | 0.0024±0.0044   |
| Coalescent depth                | 0.0027±0.0029 | 0.0033±0.0047 | 0.0018±0.0033 | 0.0009±0.0014 | 0.0038±0.0085    | 0.0040±0.0071   |
| Average intra-specific distance | 0.0014±0.0019 | 0.0021±0.0067 | 0.0010±0.0023 | 0.0008±0.0012 | 0.0015±0.0048    | 0.0033±0.0062   |
| Theta prime                     | 0.0621±0.0215 | 0.0818±0.0309 | 0.0083±0.0038 | 0.0039±0.0024 | 0.0298±0.0146    | 0.0126±0.0073   |
| Minimum inter-specific distance | 0.0611±0.0214 | 0.0799±0.0307 | 0.0078±0.0041 | 0.0036±0.0023 | 0.0286±0.0162    | 0.0122±0.0077   |
| Average inter-specific distance | 0.0618±0.0228 | 0.0790±0.0321 | 0.0087±0.0040 | 0.0041±0.0027 | 0.0295±0.0151    | 0.0120±0.0072   |

*rbcL*, respectively (Table 3). The *rbcL* region represented the lowest variable (3.67%).

### Intra- and Inter-specific Genetic Divergence of *Acer*

For all candidate barcodes, the genetic divergence was lower within species than between species (Table 4). Comparisons of the inter-specific divergence of the six barcode loci, ITS2 exhibited the highest average inter-specific distance and theta prime, followed by ITS, and the four plastid barcodes (*matK*, *rbcL*, *psbA-trnH* and *tmL-trnF*) displayed relatively lower divergence among species. In addition, minimum inter-specific distances of ITS and ITS2 regions were larger than their maximum intra-specific distances (Coalescent depth). For other candidates, the differences between minimum inter-specific variation and their maximum intra-specific variation were not so significant (Table 4).

### Barcoding Gap Assessment

The barcoding gaps between six inter- and intra-specific candidates were evaluated by graphing the distribution of genetic divergence based on the K2P model. The results indicated that ITS and ITS2 regions exhibited clear barcoding gaps, whereas the inter- and intra-specific distances of *matK*, *rbcL*, *psbA-trnH* and *tmL-trnF* were

overlapped without barcoding gaps (Fig. 1).

The significance between inter- and intra-specific K2P distances was calculated using Wilcoxon signed-rank tests. The results indicated that the intra-specific distances were lower than inter-specific distances, and ITS2 exhibited the highest variation among congeneric species, followed by ITS, while *rbcL* showed the lowest intra-specific variation (Table 5, 6). At the intra-specific level, the lowest variability was displayed by *rbcL*, and there was no significant difference in divergence between ITS and ITS2 (Table 6).

### Species Discrimination Test

Taxon DNA was applied to analyze the species identifications in *Acer* samples. Discrimination success rates varied from 16.66% (*rbcL*) to 77.77% (ITS) according to BM method, varied from 16.66% (*rbcL*) to 74.26% (ITS) according to BCM method, and varied from 25.49% (*rbcL*) to 73.09% (ITS) using the ASB method (Fig. 2). Among the six barcode candidates, ITS region turned out to have the highest identification efficiency, followed by ITS2, and *rbcL* had the lowest success rates. Additionally, *rbcL* sequence provided the highest misidentification rate in the BM and BCM analysis, and the misidentification rates of ITS and ITS2 were both lower than 10% in the BM and BCM analysis, and lower than 5% in ASB analysis.

**Table 5:** Wilcoxon signed tests for interspecific divergences of candidate sequences

| W+        | W-        | Relative Ranks                                 | Results               |
|-----------|-----------|--|-----------------------|
| ITS       | ITS2      | W+=30862.5, W-=886472.5 (n=1378, P≤3.121e-194) | ITS < ITS2            |
| ITS       | matK      | W+=245001, W-=349 (n=703, P≤1.229e-115)        | ITS > matK            |
| ITS       | rbcL      | W+=368503.5, W-=7.5 (n=861, P≤4.752e-142)      | ITS > rbcL            |
| ITS       | psbA-trnH | W+=432508.5, W-=5071.5 (n=946, P≤1.255e-147)   | ITS > psbA-trnH       |
| ITS       | trnL-trnF | W+=686287, W-=2264 (n=1176, P≤6.396e-191)      | ITS > trnL-trnF       |
| ITS2      | matK      | W+=245026, W-=324 (n=703, P≤1.131e-115)        | ITS2 > matK           |
| ITS2      | rbcL      | W+=367625, W-=28 (n=861, P≤7.554e-142)         | ITS2 > rbcL           |
| ITS2      | psbA-trnH | W+=440068.5, W-=1261.5 (n=946, P≤1.617e-153)   | ITS2 > psbA-trnH      |
| ITS2      | trnL-trnF | W+=686377, W-=2174 (n=1176, P≤5.139e-191)      | ITS2 > trnL-trnF      |
| matK      | rbcL      | W+=60661.5, W-=9089.5 (n=861, P≤6.564e-46)     | matK > rbcL           |
| matK      | psbA-trnH | W+=4055, W-=329281 (n=820, P≤8.599e-129)       | matK < psbA-trnH      |
| matK      | trnL-trnF | W+=66844, W-=264861 (n=820, P≤2.874e-49)       | matK < trnL-trnF      |
| rbcL      | psbA-trnH | W+=372, W-=565144 (n=1081, P≤5.014e-175)       | rbcL < psbA-trnH      |
| rbcL      | trnL-trnF | W+=19811, W-=561770 (n=1081, P≤8.886e-155)     | rbcL < trnL-trnF      |
| psbA-trnH | trnL-trnF | W+=834765.5, W-=41060.5 (n=1176, P≤2.665e-179) | psbA-trnH > trnL-trnF |

**Table 6:** Wilcoxon signed tests for intraspecific variations of candidate sequences

| W+        | W-        | Relative Ranks                 | Results               |
|-----------|-----------|--------------------------------|-----------------------|
| ITS       | ITS2      | W+=144, W-=156 (n=39, P≤0.864) | ITS = ITS2            |
| ITS       | matK      | W+=40, W-=26 (n=17, P≤0.534)   | ITS = matK            |
| ITS       | rbcL      | W+=100, W-=20 (n=23, P≤0.023)  | ITS > rbcL            |
| ITS       | psbA-trnH | W+=97, W-=93 (n=28, P≤0.936)   | ITS = psbA-trnH       |
| ITS       | trnL-trnF | W+=175, W-=176 (n=33, P≤0.990) | ITS = trnL-trnF       |
| ITS2      | matK      | W+=29, W-=26 (n=17, P≤0.878)   | ITS2 = matK           |
| ITS2      | rbcL      | W+=65, W-=13 (n=23, P≤0.041)   | ITS2 > rbcL           |
| ITS2      | psbA-trnH | W+=44, W-=61 (n=28, P≤0.594)   | ITS2 = psbA-trnH      |
| ITS2      | trnL-trnF | W+=121, W-=132 (n=33, P≤0.858) | ITS2 = trnL-trnF      |
| matK      | rbcL      | W+=28, W-=17 (n=17, P≤0.514)   | matK = rbcL           |
| matK      | psbA-trnH | W+=23, W-=55 (n=18, P≤0.209)   | matK = psbA-trnH      |
| matK      | trnL-trnF | W+=18, W-=60 (n=17, P≤0.099)   | matK = trnL-trnF      |
| rbcL      | psbA-trnH | W+=21, W-=70 (n=25, P≤0.087)   | rbcL = psbA-trnH      |
| rbcL      | trnL-trnF | W+=57, W-=48 (n=27, P≤0.778)   | rbcL = trnL-trnF      |
| psbA-trnH | trnL-trnF | W+=111, W-=79 (n=28, P≤0.520)  | psbA-trnH = trnL-trnF |

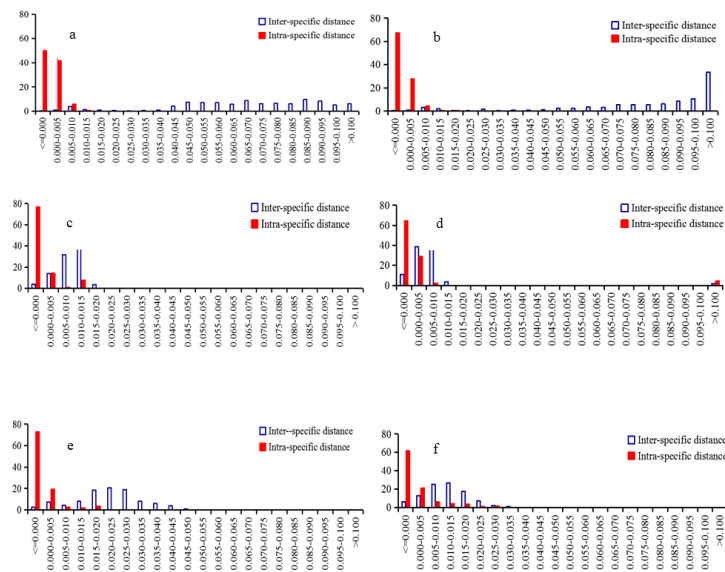


**Fig. 1:** Relative distribution of inter-specific and intra-specific K2P distances among *Acer* samples of the six barcodes. (a) ITS, (b) ITS2, (c) matK, (d) rbcL, (e) psbA-trnH, (f) trnL-trnF

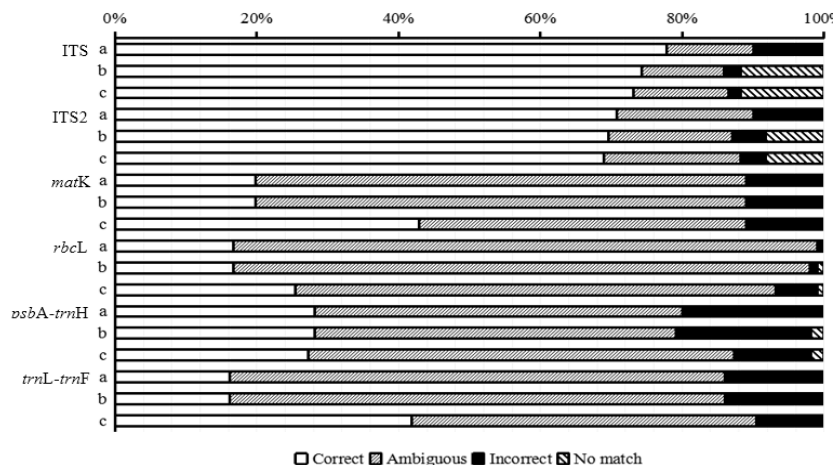


**Fig. 2:** Performance of the six barcodes based on the analysis of BM (a), BCM (b), and ASB (c). The distance threshold for BCM and ASB was computed from the intra-specific distances at 5% distances cut-off

### Phylogenetic Analysis

To put the potential barcodes assessed by Taxon DNA into perspective, ITS region that provided the highest success rate in *Acer* species discrimination (77.77 and 74.26% in the BM and BCM analysis, respectively) (Table S2) was selected for constructing phylogenetic trees. According to the *Acer* species classification system reported in Flora of China (Xu et al., 2013), all *Acer* species were classified into 14 sections, in addition to some species without grouping, such as *A. campestre*, *A. saccharum*, and *A. capillipes*. In the present study, ML tree was constructed based on 171 ITS sequences from 51 *Acer* species, which were grouped into twelve sections (*Palmata*, *Macrantha*, *Arguta*, *Negundo*, *Spicata*, *Platanoidea*, *Lithocarpa*, *Acer*, *Ginnala*, *Pentaphylla*, *Trifoliata*, and *Oblonga*), and all these samples were grouped into four main clusters (Fig. 3). Group I comprised 19 species from five sections, which was further divided into four subgroups. Except for *A. crassum*, all species belonging to sect. *Palmata* were included into subgroup I-1. *A. wardii*, a species from sect. *Macrantha*, was also included into subgroup I-1. Two species (*A. stachyophyllum* and *A. stachyophyllum* ssp. *betulifolium*) in sect. *Spicata* were clustered into subgroup I-2. The species from sect. *Negundo* and *Spicata* were grouped into subgroup I-3 and subgroup I-4, respectively. Group II contained 18 species, all species from sect. *Platanoidea* were classified into subgroup II-1, four species (*A. sinopurpurascens*, *A. tsinglingense*, *A. sterculiaceum* subsp. *franchetii* and *A. kungshanense*) from sect. *Platanoidea* were included into subgroup II-2, and all species in sect. *Macrantha* were grouped into subgroup II-2 except for *A. wardii* in subgroup I-1. Four species were clustered into group III. Subgroup III-1 included two species, one from sect. *Lithocarpa* and another one from sect. *Acer*, subgroup III-2 contained two species (*A. tataricum* subsp. *ginnala* and *A. tataricum* subsp. *semenovii*) from sect.

*Ginnala*. In addition to one species (*A. crassum*) from sect. *Palmata*, all species from other three sections were classified into Group IV. *A. pentaphyllum* constituted a separate subgroup IV-1. Three species (*A. griseum*, *A. nikoense*, and *A. triflorum*) from sect. *Trifoliata* were grouped into subgroup IV-2. Subgroup IV-3 contained six species from three sections: one from sect. *Trifoliata*, one from sect. *Palmata*, and other four from sect. *Oblonga*.

### Discussion

DNA barcode has been proved as an effective tool for species discrimination, though some experts still have doubts about its utility (Kress et al., 2005; Yu et al., 2011a). In animals, *COI* gene was established as the universal barcode (Hebert et al., 2003a; Luo et al., 2010). In plants, the standard DNA barcode have not yet been available (Yu et al., 2011a). However, several DNA regions have been proved effective for some plant taxa identification (Kress et al., 2005; Chen et al., 2010; Lee et al., 2016). In this study, six DNA sequences (ITS, ITS2, *matK*, *rbcL*, *psbA-trnH* and *trnL-trnF*) were assessed as candidate DNA barcodes in *Acer*. Considering the sequencing efficiency and quality, *rbcL* and *matK* performed better than other sequences (Table 3), which were also the two most widely accepted potential barcodes (Wang et al., 2016; Asahina et al., 2010), whereas the low substitution rates led to the low discrimination success in *Acer* (Tables 3, S2). Two chloroplast DNA sequences, *trnH-psbA* and *trnL-trnF*, provided more variable sites than the coding regions (*rbcL* and *matK*), and expressed higher identification success rate than them, but the ambiguous identification of which were also high (Fig. 2). Among these candidates, ITS exhibited the most effective discrimination, followed by ITS2, although their sequencing efficiency were relatively lower than others (Fig. 2; Table 3).

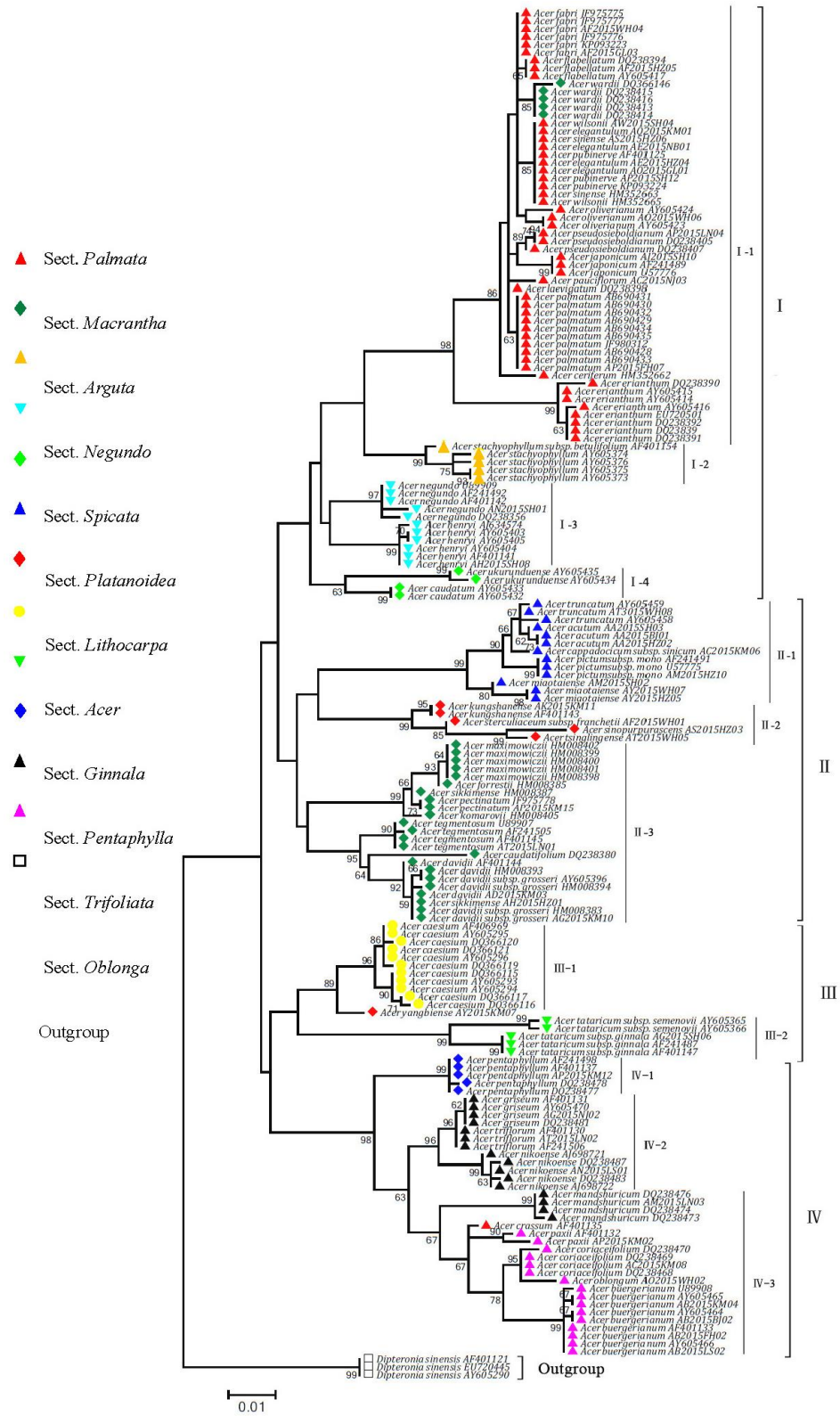


**Fig. 3:** Maximum likelihood (ML) tree based on ITS sequences for *Acer* species. Numbers above branches indicate bootstrap support (BS  $\geq$  50)

As in many previous studies (Chen *et al.*, 2008; Gao *et al.*, 2010b; Li *et al.*, 2010), ITS has been proved powerful in taxa discrimination at different levels of taxon samples. Although ITS has sometimes been deemed as an inappropriate DNA barcode for the possible impact of incomplete concerted evolution of nrDNA (Buckler and Holsford, 1996; Ren *et al.*, 2009), our study demonstrated that the possible impact may not play an important role in *Acer*. By contrast, the ITS sequence is effective in our study for its reliable discrimination capability. The ITS exhibited high genetic difference among congeneric species, which was significantly higher than the intra-specific divergence (Tables 4, 5, 6) and ITS region achieved the highest species solution percentage (in the ASB analysis) at 73.09% in *Acer*.

The ITS region cannot differentiate all the species in *Acer*. For example, *A. elegantulum*, *A. sinense* and *A. pubinerve* with identical ITS sequences were failed to be distinguished. However, more than 70% of *Acer* species could be identified using ITS locus, and the ambiguous and incorrect discrimination of ITS were the lowest, these values were relatively high for the plastid regions (Table S2). Therefore, ITS region was seemed to be the most suitable DNA barcode for *Acer* species. Additionally, some species with only one sample, the sequences of which were almost evaluated as no match; and may somewhat have resulted in a decrease in the value of correct discrimination. Hence, if taken this factor into consideration, discrimination success rates may be higher for *Acer*.

Many studies have proved that DNA barcode can not only be as a powerful tool for species-level discrimination, but also applicable for taxonomic and biodiversity studies (Tian *et al.*, 2002; Feng *et al.*, 2016; Lee *et al.*, 2016). In this study, ITS can be used to differentiate *Acer* species and serve to reconstruct phylogenetic trees in *Acer*, and 12 of Xu *et al.*'s 14 sections were supported in the trees. As reported in Fang's system (Fang, 1981), all *Acer* species were classified into two subgenera, 15 sections and 22 series, and *A. wilsonii*, *A. elegantum*, *A. sinense*, *A. olivaceum* and *A. erianthum* were grouped into sect. *Microcarpa*, *A. fabri* and *A. laevigatum* were grouped into sect. *Integrifolia*. Based on similar morphological characters such as typically palmate leaves, 4 paired bud scales, and corymbose inflorescences, De Jong (1994) and Xu *et al.* (2013) combined sect. *Palmata* and sect. *Microcarpa* into one section, sect. *Palmata*, and *A. fabri* and *A. laevigatum* were also been put in this section. Our clustering results support the classification criteria of De Jong (1994) and Xu *et al.* (2013) here. The samples of *A. negundo* and *A. henryi* were grouped together within subgroup I-3, which indicated that these two species have a close genetic relationship and it was reasonable to combined these species into sect. *Negundo* in Xu *et al.*'s system (Xu *et al.*, 2013). As shown in the ML tree, *A. yangbie* and *A. caesium* formed a monophyletic clade with high bootstrap

support (89%). However, some important morphological differences were existed between the two species, such as bud scales number, inflorescences and branchlets type. In Xu *et al.* (2013) system, *A. yangbie* was classified into sect. *Lithocarpa* rather than sect. *Acer*. Therefore, more evidence is needed for ensuring the classification status of *A. yangbie*. In addition, we found *A. wardii* was nested within species of sect. *Palmata* with relatively high bootstrap support (85%). This was backed by the study of Grimm *et al.* (2006). In the previous studies (Fang, 1996, 1981; Xu, 1996; Xu *et al.*, 2013), *A. wardii* were treated as a species of sect. *Macrantha*; while in de Jong's system, *A. wardii* was divided as a monotypic section for the uncharacteristic inflorescences (bracts, cincinni) and flowers (reflexed sepals), and this was supported by the study of Tian *et al.* (2002). In our opinion, *A. wardii* was a species worthy of further study, for its atypical morphological characteristics of sect. *Macrantha*, and for its close relationship to species of sect. *Palmata*. The species clusters also showed that the taxonomic status of *A. mandshuricum* should be revalued. *A. mandshuricum* exhibited closer relationship to sect. *Oblonga* though belonging to sect. *Trifoliata*, this was not in consensus with previously studies (Fang, 1996, 1981; Xu, 1996; Xu *et al.*, 2013). Interestingly, similar result was also found in the study of Tian *et al.* (2002).

DNA barcodes have been commonly used in species identification as complementary tool for traditional taxonomy, although some doubts on their utility still exist. DNA barcode can help non-professionals discriminate species rapidly and accurately (Luo *et al.*, 2010). In this study, six DNA barcodes for *Acer* were evaluated, and the results showed that ITS region was effective for *Acer* species identification. The ITS sequences of *Acer* species were also found having clear phylogenetic signals to resolve evolutionary relationships, and overall agreement with morphologically defined taxa (Xu *et al.*, 2013).

## Conclusion

ITS region was proved the most suitable barcode for evaluation and taxonomic implications in *Acer*, and our classification result overall agreement with morphologically-based taxa of Xu *et al.* (2013) 14 sections.

## Acknowledgements

This study is supported by grants from China Spark Programs (Grant Nos. 2015GA701004, 2015GA701016), the major project of agriculture and social development of Ningbo (Grant No. 2014C11002), the Agricultural Science and Technology Achievements Transformation Funds Project (Grant No. 2014GB2C220150), Key Scientific Research Project of Ningbo City College of Vocational Technology (Grant No. ZZX18126), and A Project Funded by the Priority Academic Program Development of Jiangsu

Higher Education Institutions. We are grateful to Yuan Zhou, Nian Wang, Yan Wei, Liwen Han, Yexin Zhang, Xuexiao Zhang, and Genguo Tang for their kind help for providing samples for this study; to Yi Song and Tao Fu for their assistance in molecular experiments and data analysis.

## References

- Asahina, H., J. Shinozaki, K. Masuda, Y. Morimitsu and M. Satake, 2010. Identification of medicinal *Dendrobium* species by phylogenetic analyses using *matK* and *rbcL* sequences. *J. Nat. Med.*, 64: 133–138
- Buckler, E.S. and T.P. Holsford, 1996. *Zea* systematics: ribosomal ITS evidence. *Mol. Biol. Evol.*, 13: 612–622
- CBOL Plant Working Group, 2009. A DNA barcode for land plants. *Proc. Natl. Acad. Sci. USA*, 106: 12794–12797
- Chen, F., H.Y. Chan, K.L. Wong, J. Wang, M.T. Yu, P.P.H. But and P.C. Shaw, 2008. Authentication of *Saussurea lappa*, an endangered medicinal material, by ITS DNA and 5S rRNA sequencing. *Planta Med.*, 74: 889–892
- Chen, S.L., H. Yao, J.P. Han, C. Liu, J. Song, L. Shi, Y. Zhu, X. Ma, T. Gao, X. Pang, K. Luo, Y. Li, X. Li, X. Jia and Y.L. Lin, 2010. Validation of the ITS2 region as a novel DNA barcode for identifying medicinal plant species. *PLoS One*, 25: e8613
- Chen, X.M., L. Yue and X.X. Huang, 2011. Analysis on the genetic relationship of *Acer trimum* L. and *Acer buergerianum* Miq. by AFLP. *Chin. Agric. Sci. Bull.*, 27: 79–83
- De Jong, P.C., 1994. Taxonomy and reproductive biology of maples. In: *Maples of the World*, pp: 69–103. Van Gelderen, D.M., P.C. de Jong and H.J. Oterdoom (eds.). Timber Press, Portland
- Fang, W.P., 1996. Revision Taxorum Aceracearum Sinicarum. *Acta Phytotax. Sin.*, 11: 139–189
- Fang, W.P., 1981. *Aceraceae*, Vol. 46, pp: 66–273. Flora Republicae Popularis Sinicae, Science Press, Beijing, China
- Feng, S., M. Jiang, Y. Shi, K. Jiao, C. Shen, J. Lu, Q. Ying and H. Wang, 2016. Application of the Ribosomal DNA ITS2 Region of *Physalis* (Solanaceae): DNA Barcoding and Phylogenetic Study. *Front. Plant Sci.*, 7: 1047
- Fay, M.F., C. Bayer, W.S. Alverson, A.Y. de Bruijn and M.W. Chase, 1998. Plastid *rbcL* sequence data indicate a close affinity between *Diegedendron* and *Bixa*. *Taxon*, 47: 43–50
- Gao, J., W.H. Meng, F. Du and J.Q. LI, 2015. DNA barcoding of *Acer palmatum* (Aceraceae). *Plant Sci. J.*, 33: 734–743
- Gao, T., H. Yao, J. Song, C. Liu, Y.J. Zhu, X.Y. Ma, X.H. Pang, H.X. Xu and S.L. Chen, 2010a. Identification of medicinal plants in the family Fabaceae using a potential DNA barcode ITS2. *J. Ethnopharmacol.*, 130: 116–121
- Gao, T., H. Yao and J. Song, 2010b. Evaluating the feasibility of using candidate DNA barcodes in discriminating species of the large Asteraceae family. *BMC Evol. Biol.*, 10: 324
- Grimm, G.W., S.S. Renner, A. Stamatakis and V. Hemleben, 2006. A nuclear ribosomal DNA phylogeny of *Acer* inferred with Maximum likelihood, splits graphs, and motif analysis of 606 sequences. *Evol. Bioinform. Online*, 2: 7–22
- Hebert, P.D.N., A. Cywinska, S.L. Ball and J. Dewaard, 2003a. Biological identifications through DNA barcodes. *Proc. R. Soc. Lond. Ser. B: Bio. Sci.*, 270: 313–321
- Hebert, P.D.N., S. Ratnasingham, S., and J.R. Dewaard, J.R., 2003b. Barcoding animal life: Cytochrome oxidase subunit 1 among closely related species. *Proc. R. Soc. Lond. Ser. B: Bio. Sci.*, 270: S96–S99
- Hebert, P.D.N. and T.R. Gregory, 2005. The promise of DNA barcoding for taxonomy. *Systemat. Biol.*, 54: 852–859
- Kress, W.J., K.J. Wurdack, E.A. Zimmer, L.A. Weig and D.H. Janzen, 2005. Use of DNA barcodes to identify flowering plants. *Proc. Natl. Acad. Sci. USA*, 102: 8369–8374
- Lee, S.Y., W.L. Ng, M.N. Mahat, M. Nazre and R. Mohamed, 2016. DNA barcoding of the endangered *Aquilaria* (Thymelaeaceae) and its application in species authentication of agarwood products traded in the market. *PLoS One*, 11: e0154631
- Li, Q.Z., X.H. Liu, J.L. Su and J. Tao, 2010. Genetic diversity of *Acer* L. germplasm revealed by sequence-related amplified polymorphism (SRAP) markers. *Jiangsu J. Agric. Sci.*, 26: 1034–1036
- Lin, L.J., L. Lin and Z.Y. Zhu, 2015. ISSR analysis of the genetic relationships among 25 *Acer* plants germplasm resources. *Guihaia (in Chinese)*, 35: 9–14
- Luo, K., S.L. Chen, K.L. Chen and Z. Liu, 2010. Assessment of candidate plant DNA barcodes using the Rutaceae family. *Sci. Chin. Life Sci.*, 53: 701–708
- Meyer, C.P. and G. Paulay, 2005. DNA barcoding: Error rates based on comprehensive sampling. *PLoS Biol.*, 3: 2229–2238
- Mora, C., D.P. Tittensor, S. Adl, A.G.B. Alastair and B. Worm, 2011. How many species are there on Earth and in the ocean? *PLoS Biol.*, 9: e1001127
- Olmstead, R.G., H.J. Michaels, K.M. Scott and J.D. Palmer, 1992. Monophyly of the Asteridae and identification of their major lineages inferred from DNA sequences of *rbcL*. *Ann. Missouri Bot. Gard.*, 79: 249–265
- Ren, B.Q., X.G. Xiang and Z.D. Chen, 2009. Species identification of *Ahnus* (Betulaceae) using nrDNA and cpDNA genetic markers. *Mol. Ecol. Resour.*, 10: 594–605
- Sang, T., D.J. Crawford and T.F. Stuessy, 1997. Chloroplast DNA phylogeny, reticulate evolution, and biogeography of *Paeonia* (Paeoniaceae). *Amer. J. Bot.*, 84: 1120–1136
- Sipe, T.W. and A.R. Linnerooth, 1995. Intraspecific variation in Samara morphology and flight behavior in *Acer saccharinum* (Aceraceae). *Amer. J. Bot.*, 82: 1412–1419
- Slabbinck, B., P. Dawyndt, M. Martens and B. De Baets, 2008. Taxon gap: a visualization tool for intra- and inter-species variation among individual biomarkers. *Bioinformatics*, 24: 866–867
- Tamura, K., G. Stecher, D. Peterson, A. Filipski and S. Kumar, 2013. MEGA6: Molecular Evolutionary Genetics Analysis version 6.0. *Mol. Biol. Evol.*, 30: 2725–2729
- Tanai, T., 1978. Taxonomical investigation of the living species of the genus *Acer* L., based on vein architecture of leaves. *J. Fac. Sci. Hokkaido Univ.*, 18: 243–282
- Tian, X., Z.H. Guo and D.Z. LI, 2002. Phylogeny of Aceraceae based on ITS and *trnL-F* data sets. *Acta Bot. Sin.*, 44: 714–724
- Tate, J.A. and B.B. Simpson, 2003. Paraphyly of *Tarasa* (Malvaceae) and diverse origins of the polyploid species. *Syst. Bot.*, 28: 723–737
- Tung, N.H., Y. Ding, S.K. Kim, K. Bae and Y.H. Kim, 2008. Total peroxyl radical-scavenging capacity of the chemical components from the stems of *Acer tegmentosum maxim.* *J. Agric. Food Chem.*, 56: 10510–10514
- Vences, M., M. Thomas, R.M. Bonett and D.R. Vieites, 2005. Deciphering amphibian diversity through DNA barcoding: chances and challenges. *Phil. Trans. Royal Soc. Lond. B: Biol. Sci.*, 360: 1859–1868
- Wang, P., X.N. Zhang, N. Tang, J. Liu, L. Xu and K. Wang, 2016. Phylogeography of *Libanotis buchtormensis* (Umbelliferae) in Disjunct Populations along the Deserts in Northwest China. *PLoS One*, 11: e0159790
- White, T.J., T. Bruns, S. Lee and J. Taylor, 1990. Amplification and direct sequencing of fungal ribosomal RNA genes for phylogenetics. In: *PCR Protocols: A Guide to Methods and Application*, pp: 315–322. Innis, M.A., D.H. Gelfand, J.J. Sninsky and T.J. White (eds.). Academic Press, New York
- Wyler, S.C. and Y. Naciri, 2016. Evolutionary histories determine DNA barcoding success in vascular plants: seven case studies using intraspecific broad sampling of closely related species. *BMC Evol. Biol.*, 16: 103
- Xu, T.Z., 1996a. Samara shape of Aceraceae and its implication in systematics and evolution. *Guihaia (in Chinese)*, 16: 109–122
- Xu, T.Z., 1996b. A new system of the genus *Acer*. *Acta Bot. Yunnan (in Chinese)*, 18: 277–292
- Xu, T.Z., 1998. The systematic evolution and distribution of the Genus *Acer*. *Acta Bot. Yunnan (in Chinese)*, 20: 383–393
- Xu, T.Z., Y.S. Chen, P.C. de Jong, H.J. Oterdoom and C.S. Chang, 2013. *Aceraceae*, Vol. 11, pp: 515–553. Flora of China, Science Press, Beijing, China

- Yao, H., J.Y. Song, C. Liu and S.L. Chen, 2010. Use of ITS2 region as the universal DNA barcode for plants and animals. *PloS One*, 5: e13102
- Yu, W.B., P.H. Huang, H. Richard, M.L. Liu, D.Z. Li and H. WANG, 2011a. DNA barcoding of *Pedicularis* L. (Orobanchaceae): Evaluating four universal barcode loci in a large and hemiparasitic genus. *J. Syst. Evol.*, 49: 425–437
- Yu, J., J.H. Xue and S.L. Zhou, 2011b. New universal matK primers for DNA barcoding angiosperms. *J. Syst. Evol.*, 49: 176–181
- Yuan, T., C.P. Wan, A. Gonzalez-Sarrias, V. Kandhi, N.B. Cech and N.P. Seeram, 2011. Phenolic Glycosides from Sugar Maple (*Acer saccharum*) Bark. *J. Nat. Prod.*, 74: 2472–2476

**(Received 12 November 2018; Accepted 08 December 2018)**